

A New Approach for Piezoelectricity Problems with Circular Inclusions

求解含圓形夾雜壓電問題之新方法

An-Chien Wu¹ Jeng-Tzong Chen²

¹Graduate Student, Department of Harbor and River Engineering

²Distinguished Professor, Department of Harbor and River Engineering

National Taiwan Ocean University

Abstract

In this paper, we derive the null-field integral equation for piezoelectricity problems with circular inclusions under remote anti-plane shears and in-plane electric fields in two directions. To fully capture circular geometries, separable expressions of fundamental solutions in the polar coordinate for field and source points and Fourier series for boundary densities are adopted to ensure the exponential convergence. Four gains are obtained, (1) well-posed model, (2) singularity free, (3) boundary-layer effect free and (4) exponential convergence. The solution is formulated in a manner of semi-analytical form since error purely attributes to the truncation of Fourier series. Problems with two piezoelectric inclusions for stress and electric displacement distributions are revisited to demonstrate the validity of our method. The main feature of the present paper is that the new formulation can be generalized to multiple circular inclusions in a straightforward way without any difficulty.

Keywords: anti-plane deformation, null-field integral equation, degenerate kernel, Fourier series, circular inclusion, piezoelectricity, Laplace problem

摘要

本文使用零場積分方程式，求解同時受反平面剪力及平面電場之含圓形夾雜壓電問題。為了充分利用圓形邊界的特性，將基本解及邊界物理量分別展開成退化核及傅立葉級數的形式；因此可以得到四個好處：矩陣良態模式、避免奇異積分、沒有邊界層效應、指數收斂。由於誤差僅來自於擷取有限項的傅立葉級數，故本方法可視為半解析法。文中求解含兩圓形夾雜之應力與電位移分布，以示範驗證本方法的有效性。本方法最大的特色是，可以直接廣泛地求解含多圓形夾雜之壓電問題。

關鍵字: 反平面位移，零場積分方程式，退化核，傅立葉級數，圓形夾雜，壓電力學，拉普拉斯方程式

Introduction

The recent technological developments and the increasing market demand have opened promising research opportunities and engineering priorities in the field of micromechanics. Coupled electro-elastic analysis in smart composites and micro-electro-mechanical systems (MEMS) receives much attention. Due to the intrinsic coupling effect of electrical and mechanical fields, the piezoelectric material is widely applied to intelligent structures. Regarding the piezoelectric circular inclusions, an exact solution of a single inclusion was derived by Pak¹ under remote anti-plane shear and in-plane electric loadings. For the two piezoelectric inclusions, Honein *et al.*² employed the Möbius transformation to derive the electromechanical field. Based on the method of analytical continuation and the techniques of successive approximation, Chao and Chang³ revisited the problem of two piezoelectric inclusions. Wu and Funami⁴ also solved this problem by using the conformal mapping and the theorem of analytical continuation. Wang and Shen⁵ considered the shear and electric loadings in two directions. Chen and Wu⁶ have successfully solved the anti-plane piezoelectricity problems with circular inclusions using the null-field integral equation in conjunction with degenerate kernels and Fourier series. Degenerate kernels play an important role⁷ not only for mathematical analysis but also for numerical implementation. For example, the spurious eigenvalue, fictitious frequency and degenerate scale have been mathematically and numerically studied by using degenerate kernels for problems with circular boundaries. One gain is that exponential convergence instead of algebraic convergence in boundary element method (BEM) can be achieved using the degenerate kernel and Fourier expansion⁸. In this paper, we revisited the problem of two piezoelectric circular inclusions which has been solved by Wu and Funami⁴ to demonstrate the generality and validity of present method.

Problem statement of anti-plane displacement field and in-plane electric potential

The physical problem to be considered is shown in Fig. 1 (a), where multiple circular inclusions are imbedded in an infinite piezoelectric medium under the far-field antiplane shear σ_{zx}^∞ , σ_{zy}^∞ and the far-field inplane electric field E_x^∞ , E_y^∞ . Bleustein⁹ has found that if one takes the plane normal to poling direction as the plane of interest, only the anti-plane displacement w couples with the in-plane electric field E_r and E_θ . Therefore, we only consider the anti-plane displacement and the in-plane electric potential such that

$$u = v = 0, \quad w = w(r, \theta); \quad E_r = E_r(r, \theta), \quad E_\theta = E_\theta(r, \theta), \quad E_z = 0, \quad (1)$$

where u , v and E_z are the vanishing components of displacements and electric field, respectively. The governing equation, in the absence of body forces and body charges, can be decoupled and simplified to

$$\nabla^2 w = 0, \quad \nabla^2 \Phi = 0, \quad (2)$$

where ∇^2 is the two-dimensional Laplacian operator

$$\nabla^2 \equiv \frac{\partial}{\partial r^2} + \frac{1}{r} \frac{\partial}{\partial r} + \frac{1}{r^2} \frac{\partial}{\partial \theta^2}, \quad (3)$$

and Φ is the in-plane electric potential. The coupling between the elastic field and the electrical field occurs only through the constitutive equations

$$\sigma_{zr} = c_{44}\gamma_{zr} - e_{15}E_r, \quad \sigma_{z\theta} = c_{44}\gamma_{z\theta} - e_{15}E_\theta, \quad (4)$$

$$D_r = e_{15}\gamma_{zr} + \varepsilon_{11}E_r, \quad D_\theta = e_{15}\gamma_{z\theta} + \varepsilon_{11}E_\theta, \quad (5)$$

where c_{44} is the elastic modulus, e_{15} is the piezoelectric constant, ε_{11} is the dielectric constant, σ_{ij} and D_i are respectively the anti-plane shear stress and in-plane electric displacement, γ_{ij} and E_i are respectively the anti-plane shear strain and in-plane electric field, which are defined as

$$\gamma_{zr} = \frac{\partial w}{\partial r}, \quad \gamma_{z\theta} = \frac{1}{r} \frac{\partial w}{\partial \theta}, \quad E_r = -\frac{\partial \Phi}{\partial r}, \quad E_\theta = -\frac{1}{r} \frac{\partial \Phi}{\partial \theta}. \quad (6)$$

By taking free body along the interface between the matrix and inclusions, the problem can be decomposed into two systems. One is an infinite medium with N circular holes under remote anti-plane shear and in-plane electric loadings as shown in Fig. 1 (b). The other is N circular inclusions bounded by the B_k contour which satisfies the Laplace equation as shown in Fig. 1 (c). From the numerical point of view, this is the so-called multi-domain approach. For the problem in Fig. 1 (b), it can be superimposed by two parts. One is an infinite medium under remote shear and electric loadings and the other is an infinite medium with N circular holes which satisfies the Laplace equation as shown in Figs. 1 (d) and 1 (e), respectively. Therefore, one exterior problem for the matrix is shown in Fig. 1 (e) and several interior problems for nonoverlapping inclusions are shown in Fig. 1 (c). The two problems in Figs. 1 (e) and 1 (c) can be solved in a unified manner since they both satisfy the Laplace equation. When the coupled effect between the mechanical and electrical fields is absent or the piezoelectric constant are equal to zero, the expressions of the electro-elastic field in the present formulation reduces to the results given by Emets and Onofrichuk¹⁰ and Chen *et al.*^{8,11}, respectively.

A unified formulation for exterior and interior Laplace problems under anti-plane mechanical and in-plane electrical loadings

Dual boundary integral equations and dual null-field integral equations

The boundary integral equation (BIE) for the domain point can be derived from the third Green's identity¹², we have

$$2\pi w(x) = \int_B T(s, x)w(s)dB(s) - \int_B U(s, x)t(s)dB(s), \quad x \in D, \quad (7)$$

$$2\pi \frac{\partial w(x)}{\partial n_x} = \int_B M(s, x)w(s)dB(s) - \int_B L(s, x)t(s)dB(s), \quad x \in D, \quad (8)$$

where $w(x)$ is the anti-plane displacement field, $t(s) = \partial w(s)/\partial n_s$, s and x are the source and field points, respectively, B is the boundary, D is the domain of interest, n_s and n_x denote the outward normal vector at the source point s and field point x , respectively, and the kernel function

$U(s, x) = \ln r$, ($r \equiv |x - s|$), is the fundamental solution which satisfies

$$\nabla^2 U(s, x) = 2\pi\delta(x - s), \quad (9)$$

in which $\delta(x - s)$ denotes the Dirac-delta function. By collocating x outside the domain ($x \in D^c$), we obtain the dual null-field integral equations as shown below

$$0 = \int_B T(s, x)w(s)dB(s) - \int_B U(s, x)t(s)dB(s), \quad x \in D^c, \quad (10)$$

$$0 = \int_B M(s, x)w(s)dB(s) - \int_B L(s, x)t(s)dB(s), \quad x \in D^c, \quad (11)$$

where D^c is the complementary domain. Based on the separable property, the kernel function $U(s, x)$ is expanded into the degenerate form by separating the source point and field point in the polar coordinate¹³:

$$U(s, x) = \begin{cases} U^i(R, \theta; \rho, \phi) = \ln R - \sum_{m=1}^{\infty} \frac{1}{m} \left(\frac{\rho}{R}\right)^m \cos m(\theta - \phi), & R \geq \rho \\ U^e(R, \theta; \rho, \phi) = \ln \rho - \sum_{m=1}^{\infty} \frac{1}{m} \left(\frac{R}{\rho}\right)^m \cos m(\theta - \phi), & \rho > R \end{cases}, \quad (12)$$

where the superscripts “ i ” and “ e ” denote the interior ($R > \rho$) and exterior ($\rho > R$) cases, respectively. The origin of the observer system for the degenerate kernel is (0,0). By setting the origin at o for the observer system, a circle with radius R from the origin o to the source point s is plotted. If the field point x is situated inside the circular region, the degenerate kernel belongs to the interior expression of U^i ; otherwise, it is the exterior case. The other kernel functions, $T(s, x)$, $L(s, x)$ and $M(s, x)$, are defined by

$$T(s, x) \equiv \frac{\partial U(s, x)}{\partial n_s}, \quad L(s, x) \equiv \frac{\partial U(s, x)}{\partial n_x}, \quad M(s, x) \equiv \frac{\partial^2 U(s, x)}{\partial n_s \partial n_x}. \quad (13)$$

Since the potentials resulted from $T(s, x)$ and $L(s, x)$ kernels are discontinuous across the boundary, the potentials of $T(s, x)$ and $L(s, x)$ for $R \rightarrow \rho^+$ and $R \rightarrow \rho^-$ are different. Therefore, $R = \rho$ is not included for degenerate kernels of $T(s, x)$ and $L(s, x)$. For problems with the k th circular boundary, we apply the Fourier series expansions to approximate the potential w and its normal derivative t on the boundary as

$$w(s_k) = a_0^k + \sum_{n=1}^L (a_n^k \cos n\theta_k + b_n^k \sin n\theta_k), \quad s_k \in B_k, \quad k = 0, 1, 2, \dots, N, \quad (14)$$

$$t(s_k) = p_0^k + \sum_{n=1}^L (p_n^k \cos n\theta_k + q_n^k \sin n\theta_k), \quad s_k \in B_k, \quad k = 0, 1, 2, \dots, N, \quad (15)$$

where N is the number of circular inclusions, $t(s_k) = \partial w(s_k) / \partial n_s$, a_n^k , b_n^k , p_n^k and q_n^k ($n = 0, 1, 2, \dots$) are the Fourier coefficients and θ_k is the polar angle. In the real computation, only $2L + 1$ finite terms are considered where L indicates the truncated terms of Fourier series.

In the present application, both anti-plane mechanical and in-plane electrical fields are modeled by using the null-field formulation. Since the electric potential Φ also satisfies the Laplace equation, the variables w and $t(s) = \partial w(s) / \partial n_s$ in Eqs. (7), (8), (10), (11), (14) and (15) can be replaced by Φ

and $\Psi(s) = \partial\Phi(s)/\partial n_s$.

Adaptive observer system

After collocating points in the null-field integral equation, the boundary integrals through all the circular contours are required. Since the boundary integral equations are obtained through the reciprocal theorem, it is frame indifferent due to the objectivity rule such that the observer system can be adaptively to locate the origin at the center of circle in the boundary integration. The adaptive observer system is chosen to fully employ the property of degenerate kernels and Fourier series. Figures 2 (a) and 2 (b) show the boundary integration for the circular boundary in the adaptive observer system. Therefore, the origin of the observer system is located on the center of the corresponding circle under integration to entirely utilize the geometry of circular boundary for the expansion of degenerate kernels and boundary densities. The dummy variable in the circular integration is the angle (θ) instead of the radial coordinate (R). In the present applications, the anti-plane mechanical and in-plane electrical fields can both be modeled by employing the same null-field formulation.

Linear algebraic system for modeling the Laplace equation

By moving the null-field point x_j to the j th circular boundary in the limit sense for Eq. (10) in Fig. 2 (a), we have

$$0 = \sum_{k=0}^N \int_{B_k} T(R_k, \theta_k; \rho_j, \phi_j) w(R_k, \theta_k) R_k d\theta_k - \sum_{k=0}^N \int_{B_k} U(R_k, \theta_k; \rho_j, \phi_j) t(R_k, \theta_k) R_k d\theta_k, \quad x(\rho_j, \phi_j) \in D^c, \quad (16)$$

where N is the number of circular inclusions and B_0 denotes the outer boundary for the bounded domain. In case of the infinite problem, B_0 becomes B_∞ . Note that the kernels $U(s, x)$ and $T(s, x)$ are assumed in the degenerate form given by Eqs. (12) and (13), respectively, while the boundary densities w and t are expressed in terms of the Fourier series expansion forms given by Eqs. (14) and (15), respectively. Then, the integrals multiplied by separate expansion coefficients in Eq. (16) are non-singular and the limit of the null-field point to the boundary is easily implemented by using appropriate forms of degenerate kernels. Thus, the collocation point $x(\rho_j, \phi_j)$ in the discretized Eq. (16) can be considered on the boundary B_j , as well as the null-field point. In the B_k integration, we set the origin of the observer system to collocate at the center c_k to fully utilize the degenerate kernels and Fourier series. By collocating the null-field point on the boundary, the linear algebraic system is obtained:

For the exterior problem of matrix, we have

$$[\mathbf{U}^M] \{ \mathbf{t}^M - \mathbf{t}^\infty \} = [\mathbf{T}^M] \{ \mathbf{w}^M - \mathbf{w}^\infty \}, \quad (17)$$

$$[\mathbf{U}^M] \{ \mathbf{\Psi}^M - \mathbf{\Psi}^\infty \} = [\mathbf{T}^M] \{ \mathbf{\Phi}^M - \mathbf{\Phi}^\infty \}. \quad (18)$$

For the interior problem of each inclusion, we have

$$[\mathbf{U}^I]\{\mathbf{t}^I\} = [\mathbf{T}^I]\{\mathbf{w}^I\}, \quad (19)$$

$$[\mathbf{U}^I]\{\mathbf{\Psi}^I\} = [\mathbf{T}^I]\{\mathbf{\Phi}^I\}, \quad (20)$$

where the superscripts “ M ” and “ I ” denote the matrix and inclusion, respectively. $[\mathbf{U}^M]$, $[\mathbf{T}^M]$, $[\mathbf{U}^I]$ and $[\mathbf{T}^I]$ are the influence matrices with a dimension of $(N+1)(2L+1)$ by $(N+1)(2L+1)$, $\{\mathbf{w}^M\}$, $\{\mathbf{t}^M\}$, $\{\mathbf{w}^\infty\}$, $\{\mathbf{t}^\infty\}$, $\{\mathbf{\Phi}^M\}$, $\{\mathbf{\Psi}^M\}$, $\{\mathbf{\Phi}^\infty\}$, $\{\mathbf{\Psi}^\infty\}$, $\{\mathbf{w}^I\}$, $\{\mathbf{t}^I\}$, $\{\mathbf{\Phi}^I\}$ and $\{\mathbf{\Psi}^I\}$ denote the column vectors of Fourier coefficients with a dimension of $(N+1)(2L+1)$ by 1. The explicit forms can be found in the Chen and his coworkers’ paper^{6,8,11}. It is noted that $\{\mathbf{w}^\infty\}$, $\{\mathbf{t}^\infty\}$, $\{\mathbf{\Phi}^\infty\}$ and $\{\mathbf{\Psi}^\infty\}$ in Fig. 1 (d) are the displacement and traction fields due to the remote shear and electric loadings, respectively. After uniformly collocating the null-field point along the k th circular boundary, Eq. (16) can be calculated by employing the relations of trigonometric function and the orthogonal property in the real computation. Only the finite L terms are used in the summation of Eqs. (14) and (15). Two cases may be solved in a unified manner using the null-field integral formulation:

- (1) One bounded problem of circular domain in Fig. 1 (c) becomes the interior problem for each inclusion.
- (2) The other is unbounded, *i.e.*, the outer boundary B_0 in Fig. 2 (a) is B_∞ . It is the exterior problem for the matrix as shown in Fig. 1 (e).

According to the continuity of displacement and equilibrium of traction along the k th interface, we have the four constraints. For the stress field, the interface condition yields

$$w^M = w^I \quad \text{on } B_k, \quad (21)$$

$$\sigma_{zr}^M = \sigma_{zr}^I \quad \text{on } B_k. \quad (22)$$

For the electric field, the interface condition yields

$$\Phi^M = \Phi^I \quad \text{on } B_k, \quad (23)$$

$$D_r^M = D_r^I \quad \text{on } B_k. \quad (24)$$

Invoking the governing equation of piezoelectricity with proper continuity conditions, fully coupled equations are obtained. By assembling the matrices in Eqs. (17)-(20) and (21)-(24), we have

$$\begin{bmatrix} \mathbf{T}^M & -\mathbf{U}^M & \mathbf{0} & \mathbf{0} & \mathbf{0} & \mathbf{0} & \mathbf{0} & \mathbf{0} \\ \mathbf{0} & \mathbf{0} & \mathbf{T}^I & -\mathbf{U}^I & \mathbf{0} & \mathbf{0} & \mathbf{0} & \mathbf{0} \\ \mathbf{0} & \mathbf{0} & \mathbf{0} & \mathbf{0} & \mathbf{T}^M & -\mathbf{U}^M & \mathbf{0} & \mathbf{0} \\ \mathbf{0} & \mathbf{0} & \mathbf{0} & \mathbf{0} & \mathbf{0} & \mathbf{0} & \mathbf{T}^I & -\mathbf{U}^I \\ \mathbf{I} & \mathbf{0} & -\mathbf{I} & \mathbf{0} & \mathbf{0} & \mathbf{0} & \mathbf{0} & \mathbf{0} \\ \mathbf{0} & \mathbf{c}_{44}^M & \mathbf{0} & \mathbf{c}_{44}^I & \mathbf{0} & \mathbf{e}_{15}^M & \mathbf{0} & \mathbf{e}_{15}^I \\ \mathbf{0} & \mathbf{0} & \mathbf{0} & \mathbf{0} & \mathbf{I} & \mathbf{0} & -\mathbf{I} & \mathbf{0} \\ \mathbf{0} & \mathbf{e}_{15}^M & \mathbf{0} & \mathbf{e}_{15}^I & \mathbf{0} & -\mathbf{\epsilon}_{11}^M & \mathbf{0} & -\mathbf{\epsilon}_{11}^I \end{bmatrix} \begin{bmatrix} \mathbf{w}^M \\ \mathbf{t}^M \\ \mathbf{w}^I \\ \mathbf{t}^I \\ \mathbf{\Phi}^M \\ \mathbf{\Psi}^M \\ \mathbf{\Phi}^I \\ \mathbf{\Psi}^I \end{bmatrix} = \begin{bmatrix} \mathbf{a} \\ \mathbf{0} \\ \mathbf{b} \\ \mathbf{0} \\ \mathbf{0} \\ \mathbf{0} \\ \mathbf{0} \\ \mathbf{0} \end{bmatrix}, \quad (25)$$

where $\{\mathbf{a}\}$ and $\{\mathbf{b}\}$ are the forcing terms due to the far-field antiplane shear and the far-field

inplane electric field, $[\mathbf{I}]$ is an identity matrix, $[\mathbf{c}_{44}^M]$, $[\mathbf{c}_{44}^I]$, $[\mathbf{e}_{15}^M]$, $[\mathbf{e}_{15}^I]$, $[\mathbf{\epsilon}_{11}^M]$ and $[\mathbf{\epsilon}_{11}^I]$ are the diagonal matrix for each material constant. After obtaining the unknown Fourier coefficients in Eq. (25), the origin of observer system is set to c_k in the B_k integration as shown in Fig. 2 (b) to obtain the field potential by employing Eq. (7). In determining the stress and electric fields, gradient of potential should be determined with care by employing the vector decomposition technique in the hypersingular equation^{6,8,11}.

Numerical results and discussions

The exact solution for a single piezoelectric inclusion, which was derived by Pak¹, can be derived by using the present formulation. Although our formulation is general for multiple inclusions, we consider the two-inclusion problem to demonstrate the validity of present method. The radii of two piezoelectric circular inclusions are r_1 and r_2 with $r_1 = r_2$ centered on the x axis and perfectly bonded to an infinite piezoelectric matrix subjected to the remote shear and the electric field as shown in Fig. 3 (a). The distance d between the two inclusions, the applied loadings and material properties of the matrix and two inclusions are assumed as the same of Wu and Funami⁴. Figure 3 (b) shows the stress and electric displacement distributions along the contour $(1.01, \theta)$ when only the remote shear $\sigma_{zy}^\infty = \tau_\infty$ is applied. It can be seen that the electro-elastic fields σ_{zr} and D_r have an asymmetric distribution and $\sigma_{z\theta}$ and D_θ have a symmetric distribution for $\theta = \pi$. In comparison with σ_{zr} , the value of stress component $\sigma_{z\theta}$ is relatively low. Figure 3 (c) illustrate the stress and electric displacement distributions along the x axis when the electric field $E_y^\infty = E_\infty$ is applied at infinity. From this figure, it can be observed that the stress component σ_{zy} in two piezoelectric inclusions has a different sign from one in the matrix. Particularly, the stress component σ_{zy} between two piezoelectric inclusions has a large varying gradient. In comparison with the stress field, the electric displacement field has a smooth varying tendency. The present results using twenty terms of Fourier series ($L = 20$) agree very well with those of Wu and Funami⁴.

Conclusions

The present work not only demonstrated an elegant method for solving boundary value problems but also understood the interesting coupling behaviors between mechanical and electrical fields that have not been studied previously by using BIE. It was shown that the electro-elastic field depends on the distance between two piezoelectric inclusions, the mismatch in the material constants and the magnitude of mechanical and electromechanical loadings. In addition, the mechanical and electrical loadings applied at infinity also have an important effect on the distribution of the electro-elastic field. Singularity free, boundary-layer effect free, exponential convergence and well-posed model are the main gains using the present formulation.

Acknowledgments

The first author (An-Chien Wu) would like to thank the student scholarship from the China Engineering Consultants, Inc., Taiwan. This work was partially supported by the National Science Council, Taiwan, through grant no. NSC94-2211-E-019-009 to National Taiwan Ocean University.

References

1. Pak, Y.E., "Circular inclusion problem in antiplane piezoelectricity," *International Journal of Solids and structures*, Vol. 29, pp. 2403-2419 (1992).
2. Honein, T., Honein, B.V., Honein, E., and Herrmann, G., "On the interaction of two piezoelectric fibers embedded in an intelligent material," *Journal of intelligent material systems and structures*, Vol. 6, pp. 229-236 (1995).
3. Chao, C.K., and Chang, K.J., "Interacting circular inclusions in antiplane piezoelectricity," *International Journal of Solids and structures*, Vol. 36, pp. 3349-3373 (1999).
4. Wu, L.Z., and Funami, K., "The electro-elastic field of the infinite piezoelectric medium with two piezoelectric circular cylindrical inclusions," *Acta Mechanica Sinica*, Vol. 18, pp. 368-385 (2002).
5. Wang, X., and Shen, Y.P., "On double circular inclusion problem in antiplane piezoelectricity," *International Journal of Solids and Structures*, Vol. 38, pp. 4439-4461 (2001).
6. Chen, J.T., and Wu, A.C., "Null-field approach for piezoelectricity problems with arbitrary circular inclusions," *Engineering Analysis with Boundary Elements*, Accepted (2006).
7. Kress, R., *Linear integral equations*, Springer-Verlag, Berlin (1989).
8. Chen, J.T., and Wu, A.C., "Null-field approach for the multi-inclusion problem under anti-plane shear," *Journal of Applied Mechanics*, ASME, Accepted (2006).
9. Bleustein, J.L., "New surface wave in piezoelectric materials," *Applied Physics Letters*, Vol. 13, pp. 412-413 (1968).
10. Emets, Y.P., and Onofrichuk, Y.P., "Interaction forces of dielectric cylinders in electric fields," *Transactions on Dielectrics and Electrical Insulation*, IEEE, Vol. 3, pp. 87-98 (1996).
11. Chen, J.T., Shen, W.C., and Wu, A.C., "Null-field integral equations for stress field around circular holes under antiplane shear," *Engineering Analysis with Boundary Elements*, Vol. 30, pp. 205-217 (2006).
12. Chen, J.T., and Hong, H-K., "Review of dual boundary element methods with emphasis on hypersingular integrals and divergent series," *Applied Mechanics Reviews*, ASME, Vol. 52, pp. 17-33 (1999).
13. Chen, J.T., and Chiu, Y.P., "On the pseudo-differential operators in the dual boundary integral equations using degenerate kernels and circulants," *Engineering Analysis with Boundary Elements*, Vol. 26, pp. 41-53 (2002).

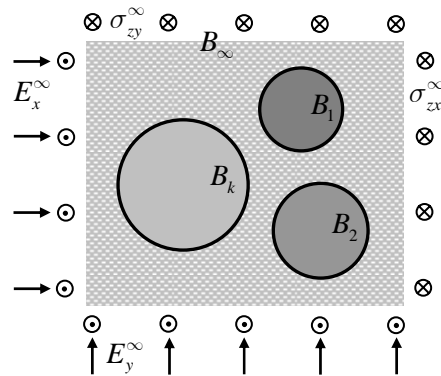


Figure 1 (a) Infinite anti-plane piezoelectricity problem with arbitrary piezoelectric circular inclusions under remote shear and electric loadings.

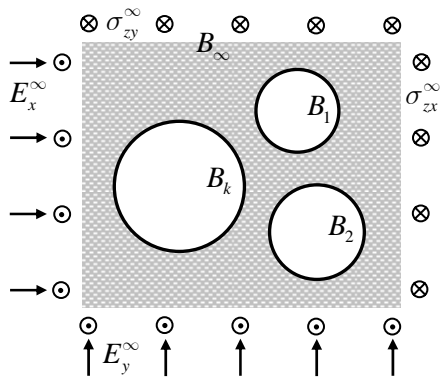


Figure 1 (b) Infinite piezoelectric medium with circular holes under remote shear and electric loadings.

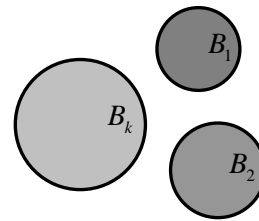


Figure 1 (c) Interior Laplace problems for each piezoelectric circular inclusion.

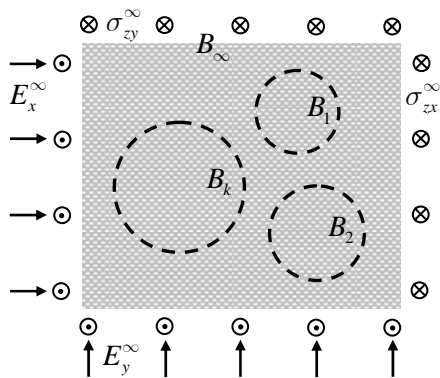


Figure 1 (d) Infinite piezoelectric medium under remote shear and electric loadings.

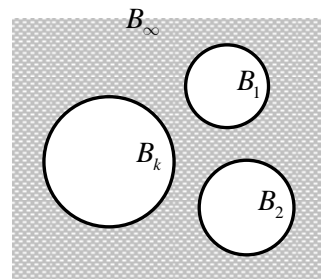


Figure 1 (e) Exterior Laplace problems for the piezoelectric medium.

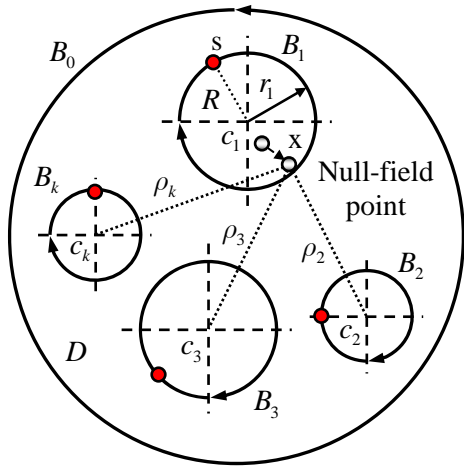


Figure 2 (a) Sketch of the null-field integral equation for a null-field point in conjunction with the adaptive observer system ($x \notin D, x \rightarrow B_k$).

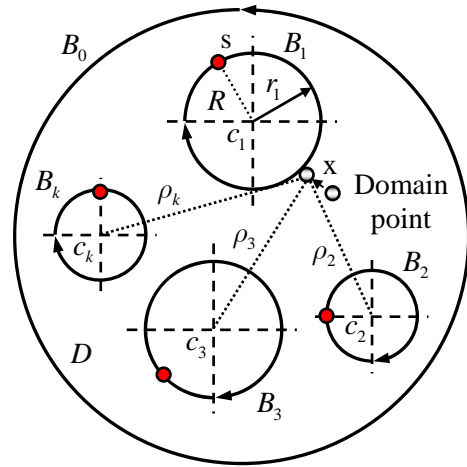


Figure 2 (b) Sketch of the boundary integral equation for a domain point in conjunction with the adaptive observer system ($x \in D, x \rightarrow B_k$).

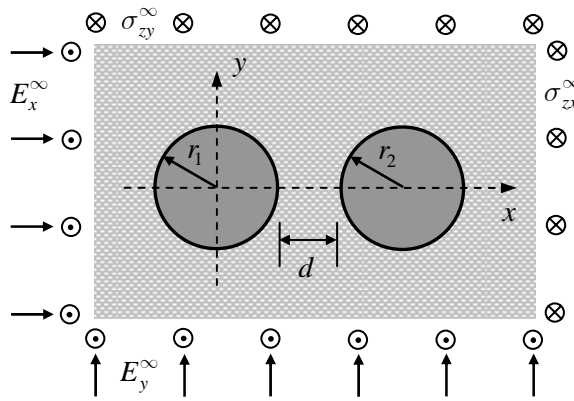


Figure 3 (a) Two circular inclusions embedded in a matrix under remote shears and electric fields.

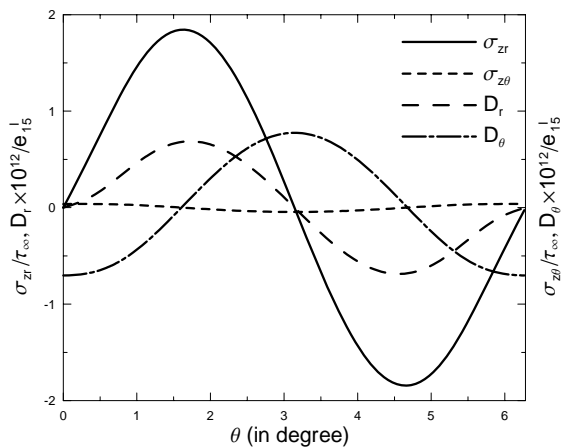


Figure 3 (b) Stress and electric displacement distributions along the contour ($1.01, \theta$) when $d = 1.5r_1, \sigma_{zy}^\infty = \tau_\infty$.

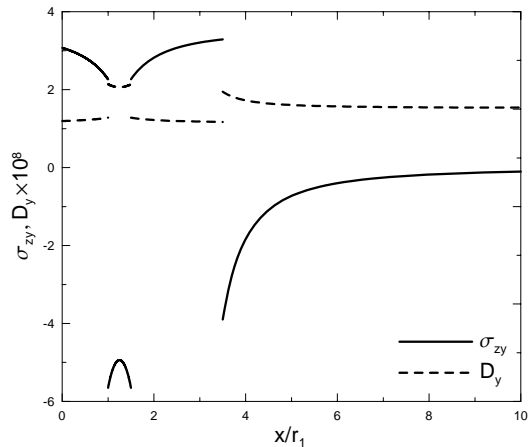


Figure 3 (c) Stress and electric displacement distributions along the x axis when $d = 0.5r_1, E_y^\infty = E_\infty$.